

REPORT DOCUMENTATION PAGE*Form Approved*
OMB No. 0704-0188

Public reporting burden for this collection of information is estimated to average 1 hour per response, including the time for reviewing instructions, searching data sources, gathering and maintaining the data needed, and completing and reviewing the collection of information. Send comments regarding this burden estimate or any other aspect of this collection of information, including suggestions for reducing this burden to Washington Headquarters Service, Directorate for Information Operations and Reports, 1215 Jefferson Davis Highway, Suite 1204, Arlington, VA 22202-4302, and to the Office of Management and Budget, Paperwork Reduction Project (0704-0188) Washington, DC 20503.

PLEASE DO NOT RETURN YOUR FORM TO THE ABOVE ADDRESS.

1. REPORT DATE (DD-MM-YYYY) NOV 08			2. REPORT TYPE Conference Paper Postprint		3. DATES COVERED (From - To) Oct 05 – Oct 07	
4. TITLE AND SUBTITLE DESIGN AND DEVELOPMENT OF A PACKAGE FOR A DILUTED WAVEGUIDE ELECTRO-ABSORPTION MODULATOR				5a. CONTRACT NUMBER In-House		
				5b. GRANT NUMBER		
				5c. PROGRAM ELEMENT NUMBER 62702F		
6. AUTHOR(S) S. Tan, N. Stoffela, C. Shick, T. McDonald, A. Whitbeck, R. Erdmann, R. Michalak, R. Bussajer, I. Shubin and P. Yu				5d. PROJECT NUMBER SEMI		
				5e. TASK NUMBER SN		
				5f. WORK UNIT NUMBER 01		
7. PERFORMING ORGANIZATION NAME(S) AND ADDRESS(ES) AFRL/RYP 25 Electronics Pkwy Rome NY 13441-4505				8. PERFORMING ORGANIZATION REPORT NUMBER		
9. SPONSORING/MONITORING AGENCY NAME(S) AND ADDRESS(ES) AFRL/RYP 25 Electronics Pkwy Rome NY 13441-4505				10. SPONSOR/MONITOR'S ACRONYM(S)		
				11. SPONSORING/MONITORING AGENCY REPORT NUMBER AFRL-RY-RS-TP-2008-7		
12. DISTRIBUTION AVAILABILITY STATEMENT Approved for public release; distribution unlimited. PA# AFRL WS 07-0388						
13. SUPPLEMENTARY NOTES Paper published in Proc. of SPIE Vol 6975, 69750O. This material is declared a work of the U. S. Government and is not subject to copyright protection in the United States.						
14. ABSTRACT Externally coupled electro-absorption modulators (EAM) are commonly used in order to transmit Radio-Frequency (RF) signals on optical fibers. Recently an alternative device design with diluted waveguide structures has been developed. Bench tests show benefits of lower propagation loss, higher power handling (100 mW), and higher normalized slope efficiency. This paper addresses the specific issues involved in packaging the diluted waveguide EAM devices. An evaluation of the device requirements was done relative to the standard processes. Bench tests were performed in order to characterize the optical coupling of the EAM. The photo current maximum was offset from the optical power output maximum. The transmissions vs bias voltage curves were measured, and an XY scanner was used to record the mode field of the light exiting from the EAM waveguide in each position. The Beam Propagation Method was used to simulate the mode field and the coupling efficiency. A design including mechanical, optical and RF elements was developed. A Newport Laser Welding system was utilized for fiber placement and fixation.						
15. SUBJECT TERMS Electro-absorption modulator (EAM), packaging fiber coupling, dilute core waveguide (DCW), RF optical link						
16. SECURITY CLASSIFICATION OF:			17. LIMITATION OF ABSTRACT UU	18. NUMBER OF PAGES 10	19a. NAME OF RESPONSIBLE PERSON Richard Michalak	
a. REPORT U	b. ABSTRACT U	c. THIS PAGE U			19b. TELEPHONE NUMBER (Include area code) N/A	

Design and Development of a Package for a Diluted Waveguide Electro-absorption Modulator

Songsheng Tan^a, Nancy Stoffel^{a*}, Charles Shick^a, Terrance McDonald^a, Al Whitbeck^a, Reinhard Erdmann^b, Richard J Michalak^b, Rebecca Bussjager^b, Ivan Shubin^c, Paul K. L. Yu^c

^aInfotonics Technology Center, 5450 Campus Drive, Canandaigua, NY 14424

^bAir Force Research Laboratory SNBP, 25 Electronic Pkwy, Rome, NY 13441

^cUniversity of California at San Diego

ABSTRACT

Externally coupled electroabsorption modulators (EAM) are commonly used in order to transmit RF signals on optical fibers. Recently an alternative device design with diluted waveguide structures has been developed. [1] Bench tests show benefits of lower propagation loss, higher power handling (100 mW), and higher normalized slope efficiency.

This paper addresses the specific issues involved in packaging the diluted waveguide EAM devices. An evaluation of the device requirements was done relative to the standard processes. Bench tests were performed in order to characterize the optical coupling of the EAM. The photo current maximum was offset from the optical power output maximum. The transmissions vs. bias voltage curves were measured, and an XY scanner was used to record the mode field of the light exiting from the EAM waveguide in each position. The Beam Propagation Method was used to simulate the mode field and the coupling efficiency. Based on the bench tests and simulation results, a design including mechanical, optical and RF elements was developed. A Newport Laser Welding system was utilized for fiber placement and fixation. The laser welding techniques were customized in order to meet the needs of the EAM package design.

Keywords: Electroabsorption modulator (EAM), packaging, fiber coupling, dilute core waveguide (DCW), RF optical link

1. INTRODUCTION

Transmission of RF signals via optical fiber requires modulation of the output of a laser to create an RF signal. The light exiting the modulator is then coupled to a fiber for transmission. At the receiving end, the signal is detected by a photodetector and demodulated back into an electrical signal. Electroabsorption modulators have been successfully used as part of analog optical link applications in the region of 1.3 and 1.55 μm . EAMs are attractive due to their compact size, wide optical transmission bands, and potential for monolithic integration with other components. Challenges to the optimal functioning of EAMs include low optical signal loss, high slope efficiencies, and optical saturation powers.

The device studied in this paper is a dilute core waveguide (DCW) electroabsorption modulator (EAM). It was developed at UCSD and has a similar structure as that of high-saturation-power waveguide photodetector described in an earlier publication. [2] The DCW EAM was designed to enhance the optical power handling and provide a greater spur-free dynamic range relative to a more conventional EAM design. [3]. The approach used to achieve this goal was to reduce the optical confinement factor at the electroabsorption (EA) layer in order to enhance the dynamic range and the maximum power of the EAM. This approach has some interesting effects on the assembly methods which must be utilized to form a low loss packaged device.

Figure 1 is a schematic description of the DCW EAM structure. For a semiconductor PN junction, there is a depletion layer with a high electric field that serves to separate photo generated electron-hole pairs which is the source of photo current. The current DCW EAM diode is a PIN structure. The un-doped multiple quantum-well (MQW) layer with a thickness of 0.275 μm is an electroabsorption (EA) layer. The upper neighbor of this EA layer is an intrinsic-InP layer with a thickness of 0.15 μm . These two layers combined form the I Layer of the junction. Sandwiching the I layer are the P layer with a doping level of $4 \times 10^{17} \text{ cm}^{-3}$, and the N layer with a doing level of $3 \times 10^{18} \text{ cm}^{-3}$. The depletion layer of diodes should be in the I layer and be slightly extended towards the P and N layers. The implication in assembly is that the lensed fiber position, which will create a maximum of photo currents of the DCW EAM diode, will be almost at the center of the combined I layer.

The insertion loss of the EAM module is one important parameter used to characterize the assembly process. Lower insertion loss means higher optical transmission. For the conventional EAM chip, the EA layer is also the optical waveguide. Therefore the location of a lensed fiber positioned to achieve a maximum photo power will overlap with the lensed fiber positioned to produce the maximum photo current. As a result, the assembly process sequence for a conventional EAM module is to place the first fiber at the photo current maximum position of EAM diode. The second fiber will be placed in position in order to have maximum photo power output.

For the current DCW EAM chip the optical waveguide is formed by a combination of the patterned EA layers and the underlying layer of an n type InGaAsP layer. Together these layers combine to form a ridge waveguide. As shown in Figure 1, for the DCW EAM the axes for fiber placement that corresponds to the photo current maximum will be separated from the axes corresponding to the photo power maximum. The assembly process of DCW EAM should not be the same as that for the conventional EAM.

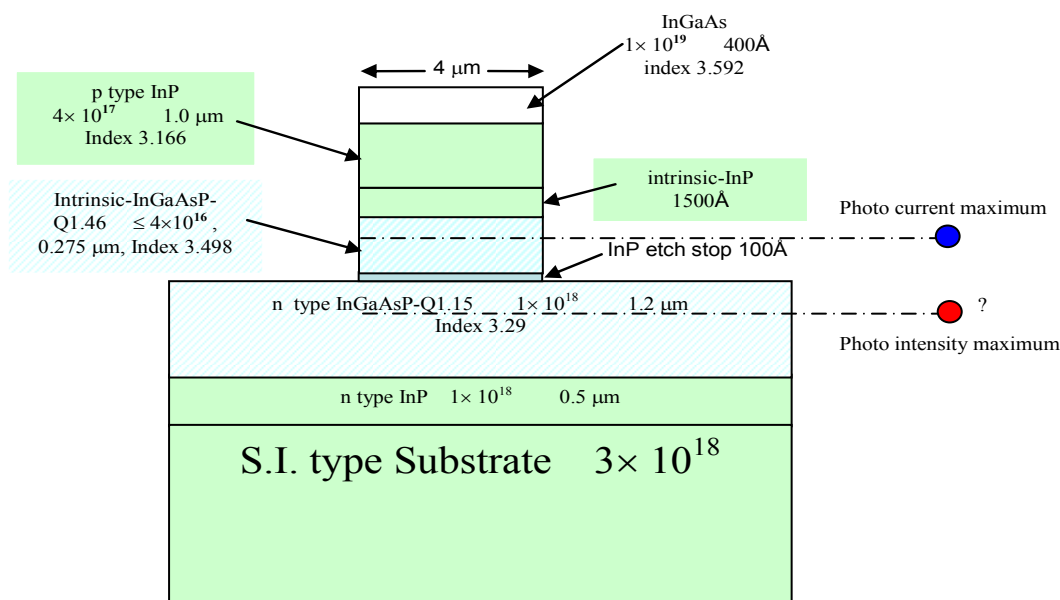


Figure 1: Schematic cross section of the DCW EAM structure

2. METHODOLOGY

2.1 Packaging Equipment

Creating an EAM assembly requires specialized tools to align and fix the input and output fibers in place, to place the device with precision, to wire bond, and to create a hermetically sealed package. In the process of packaging the device within a gold-plated Kovar dual fiber pigtail package we utilized a number of specialized pieces of equipment. The major tools included a Newport Laser Welder, Newport Fiber Auto Alignment System, ATV Solder Reflow Oven, F&K Gold Ball Bonder, K&S 626 wire Bonder, Suss FC150 Bonder, Research Devices M8 Flip Chip Bonder, SSE 2000 Seam Sealer, and Varian Fine Leak Detector System...

2.2 Mechanical Design of the EAM Module

The EAM module design is more complicated than that of an ordinary laser module. The EAM module requires optical fiber coupling with both facets of the chip, and an RF electrical connection.

A custom designed butterfly package was used with seven electrical connection pins, one RF connector, and two fiber inlets. Figure 2 is a sketch of the EAM module built at ITC, which describes the major components and the sequence of the assembly.

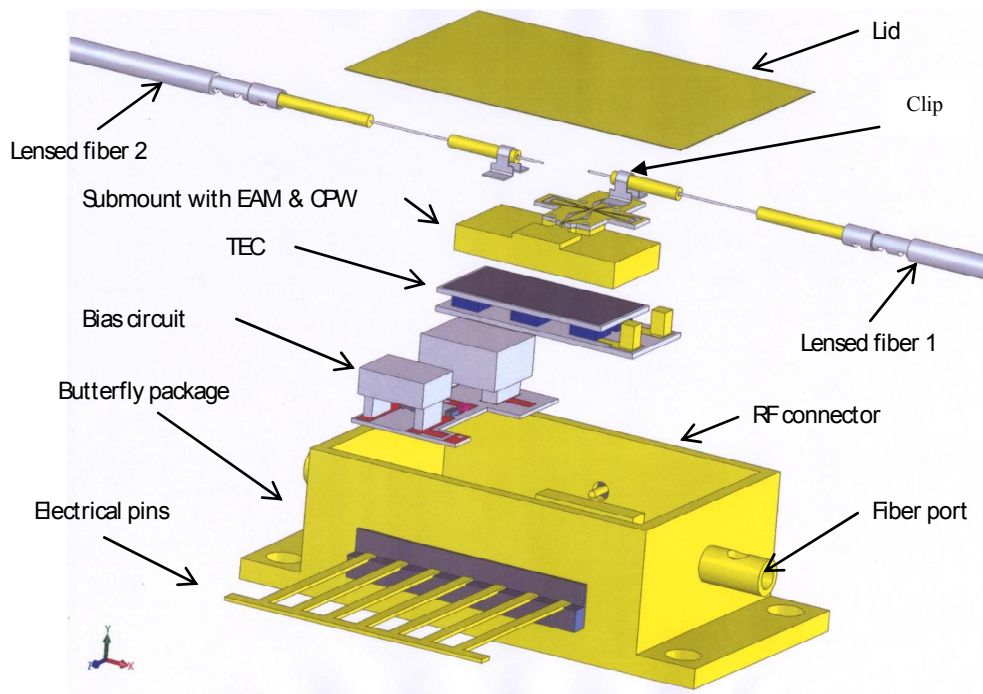


Figure 2: EAM Module Components

Two metal ferrules surround each fiber. One of the ferrules is used to fix the fiber to the submount. This is done via laser welding wherein a metal clip is placed over the ferrule. The base of the ferrule is welded to the submount, and the shoulder of the clip is welded to the ferrule. These bonds were made using the Newport laser welder. The second ferrule was located such that it will reside within the fiber port of the butterfly package. Solder were used to seal the gaps between fiber ferrule and the fiber inlet on the butterfly package. This is a similar process to that used to manufacture commercial pump laser modules. The module size, excluding the RF connector and electrical pins, is about 26L x 18W x 10H mm³.

The EAM chip is quite small, with dimensions about 300 x 200 x 150 μm^3 . Handling was made even more difficult by the necessity to avoid touching the waveguide. In order to handle the device during the assembly process we custom-designed a tool which had vacuum features to pick up the chip on the wire bond pads. This pickup tool was made out of silicon, was patterned lithographically and etched. It was used successfully in order to pick up the EAM chip and to place the EAM chip on the submount for bonding by the flip chip bonder. The result was device placement with a lateral shift tolerance of $\pm 5 \mu\text{m}$ and with an angular tolerance of $\pm 1^\circ$ as measured by the Nikon Measure Scope 20.

The electrical diagram of this EAM module is shown in Figure 3. (This schematic does not include the thermoelectric cooler and thermistor). A capacitor was used on the coplanar waveguide (CPW) as a DC block in order to prevent the DC bias voltage applied to the RF connector. A bias circuit was used to prevent the RF signal from leaking to the DC bias source.

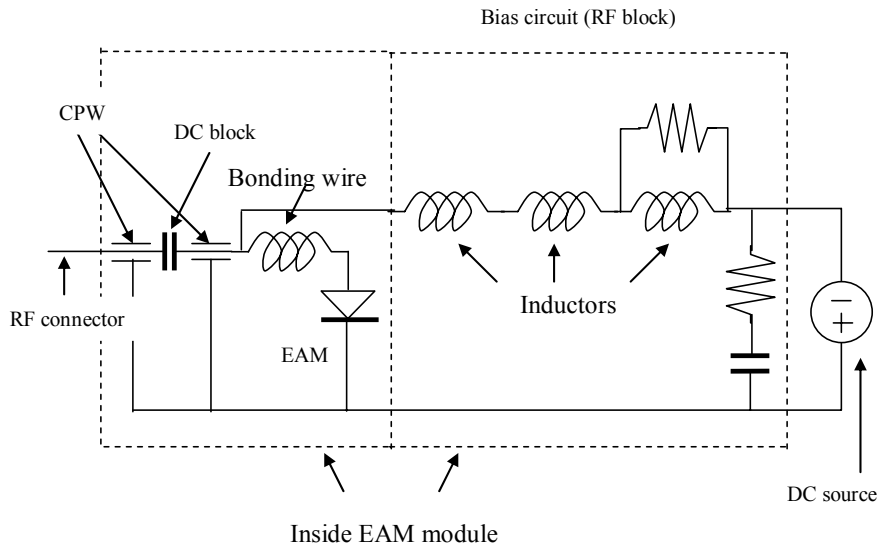


Figure 3: The electrical diagram of EAM module

In order to transition between the optical mode of the EAM waveguide and the glass fiber, an optical mode converter is necessary. Corning OptiFocus lensed fiber was used as the optical converter to improve the coupling efficiency. The mode field diameter (MFD) of this kind of lensed fiber is about $3.3 \mu\text{m}$. The choice of this particular lensed fiber in this work was only for convenience, because the vendor could provide the lensed fiber with metal ferrules. A MFD of $3.3 \mu\text{m}$ is not be the optimal in order to obtain the maximum coupling efficiency.

3. MEASUREMENT

3.1 Device characterization

As a result of the design characteristics of DCW EAM discussed in the introduction, it is necessary to find the optimum coupling position of the lensed fiber by experimental bench tests in order to develop a proper assembly process. An optical test was setup and conducted as shown in Figure 4. This is a one lensed fiber test method. The laser light output from the lensed fiber was coupled into one facet of the EAM chip. The light exiting from the other facet of the EAM chip passed through a lens and was focused on a Newport detector, which was connected to a Newport power meter to measure the photo power. Two probes were contacted to the electrical pads of the EAM. These two probes were connected to a Keithley source meter in order to apply a bias voltage and to measure the photo current. This experimental setup was built on a two stage Newport fiber alignment system. The lensed fiber was placed on one 4 axis stage, so the fiber could be scanned with a positional accuracy of 50 nm. At the same time the photo current and photo power were measured.

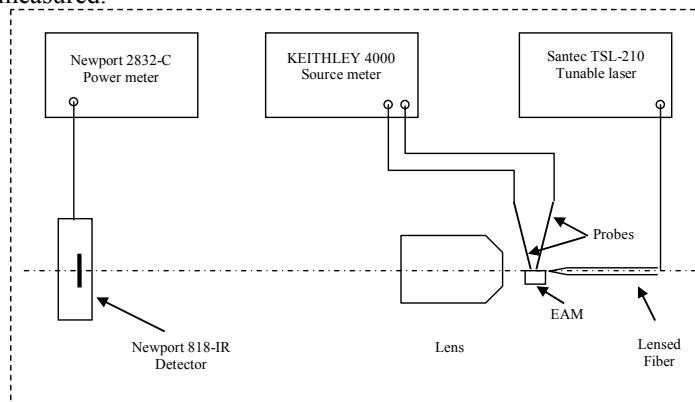


Figure 4: The sketch of the bench test

Figure 5 is a typical set of photo current and photo intensity curves produced during the bench test. The measured current was the real photo current of the EAM chip. However, the measured photo power is not the same as that exiting from the waveguide on the EAM chip since the lens system is present. If it is necessary to estimate the photo power exiting from the waveguide, the insertion loss of the optical system must be taken into account. In the bench test, the lensed fiber was first placed in the maximum photo current position and then moved up a couple of microns to reach the starting position of the test. Then the fiber was scanned down step by step in increments of about $0.2\ \mu\text{m}$ while holding the EAM chip stationary. The position of the light spot on the detector shifts somewhat during the fiber scan; therefore the height of the detector was adjusted in order to record the photo power correctly.

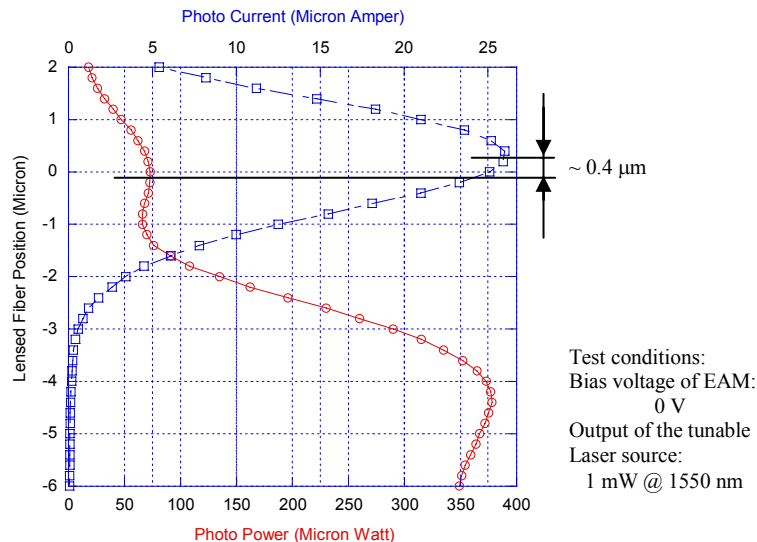


Figure 5: The photo current and photo intensity curves of DCW EAM

There are two peaks observed on the photo power curve: the lower power peak and the higher power peak. Normalized transfer curves were measured at these two peak positions as shown in Figure 6. The electroabsorption function of the DCW EAM chip was observed at the lower power peak position, but not at the higher power peak position. It seems the lower power peak position is the real fiber position for the DCW EAM module and is referred to as the photo power maximum in this paper. The higher power peak position is too far away from the EA layer to have any electroabsorption effect. Instead the higher power peak was due to transmission through the InP substrate similar to that observed on the ordinary Si ridge waveguide.

Comparing the positions between the photo current maximum and the photo power maximum in Figure 5, it was found there was a separation with a distance of about $0.4\ \mu\text{m}$. The test results indicate that the EA layer and the optical waveguide of DCW EAM are really decoupled. The light entering the EAM chip was confined by the ridge waveguide; composed of both the i-InGaAsP and n-InGaAsP layers.

3.2 Fiber coupling methodology

A modified EAM assembly process was developed based on the photo current and photointensity curves of the DCW EAM. The input fiber was first placed at the photo current maximum position and then scanned down a specific distance. For each device, the adjustment in height was determined by a bench test for each EAM chip before final assembly. The second lensed fiber was placed at the position which yielded a maximum photo power output.

After laser welding, the fiber position shifts slightly due to thermal expansion effects. A custom designed re-bending system was used to move the fiber back into a more optimal position. During the rebend process the back side of the first metal ferrule on the lensed fiber was held. Since the first metal ferrule has been welded on the clip, the movement of the holder in vertical and horizontal directions will rotate the tip of the fiber and hence provide adjustments in lateral and vertical directions. The process continued until levels of photopower and photocurrent were achieved similar to the values achieved in the pretest.

The rebend process was an important step in maximizing the coupling for the DCW EAM. During the placement of the first lensed fiber, it is only possible to monitor the photo current. Since the correct position of the first lensed fiber

was not at the photo current maximum, the 0.4 μm shift of the fiber could not insure the first lensed fiber was at the optimum position. So fine-tuning of the first lensed fiber placement was necessary after the placement of the second lensed fiber and was accomplished using the rebending system.

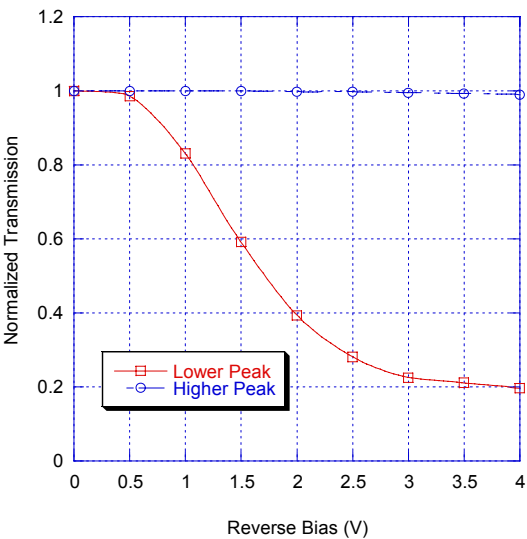


Figure 6: Extinction curves of the DCW EAM at two peak positions

3.3 Optical Mode Profiling of DCW EAM

An XY BeamScan was used to measure the far view (diverse angle of the beam) and the near view (optical mode) of the DCW EAM chip. When the BeamScan head was placed very near the light exit point of the chip, the diverse angle of the light beam can be calculated by (BeamScan width)/Distance. Table 1 lists the diverse angle of light beam exiting from the Corning OptiFocus lensed fiber and the DCW EAM. The near view measurement used a similar optical system as shown in Figure 4. The BeamScan head was used instead of the detector. A calibration of the magnification of the optical system was performed in order to properly interpret the measured data. Figure 7 is the near view measurement of DCW EAM by BeamScan. The BeamScan profile shows that the mode field of the DCW EAM is almost circular and is about 3.7 μm in diameter. This is in contrast to the mode field of the Corning OptiFocus lensed fiber used in the assembly process which had a mode field of 3.3 μm .

Table 1: The far view of the lensed fiber and EAM chip

Sample	FWHM (in degree)	
	In Horizontal	In Vertical
Lensed fiber	41.2°	41.6°
DCW EAM	53.0°	52.6°

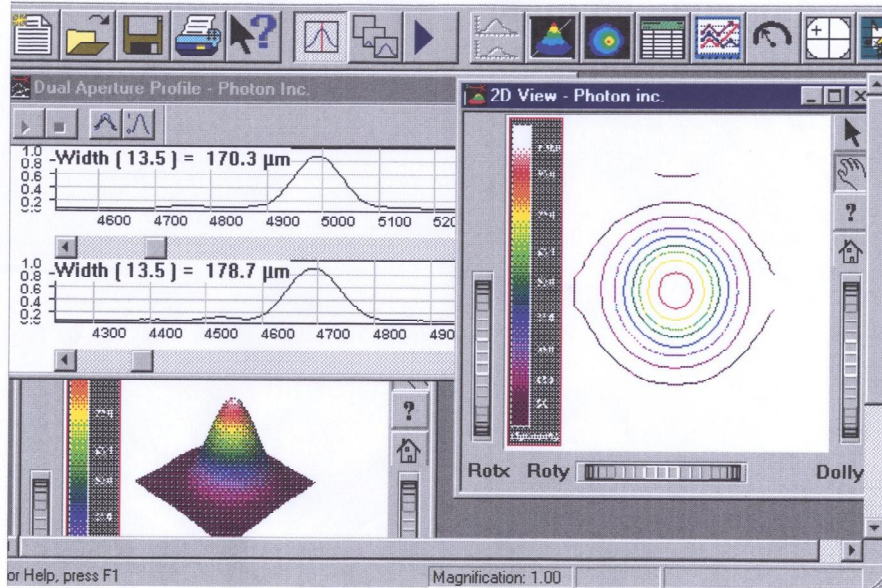


Figure 7: The BeamScan profile of near view of DCW EAM chip

A coupling test was conducted by using one lensed fiber test method. The lensed fibers with a mode field of $3.3\ \mu\text{m}$ and $4\ \mu\text{m}$ were used in this test. It was found that the coupling efficiency is higher for the lensed fiber with the mode field of $4\ \mu\text{m}$. The coupling efficiency ratio between lensed fiber with mode field of $4\ \mu\text{m}$ and lensed fiber with mode field of $3.3\ \mu\text{m}$ was about 1.17 estimated by the photo current ratio and the photo power ratio. This coupling test results matches with the BeamScan measurement of mode field diameter of $3.7\ \mu\text{m}$.

4. MODULE PERFORMANCE

The test results for six dual fiber butterfly packages are listed in Table 2. Figure 8 is a top view photograph of the EAM module. The major components inside the module can be identified by comparison with Figure 2. Table 2 lists the measured insertion loss before and after assembly. It was found that an extra insertion loss of about 1.2 db was created during the assembly process. Module 27 has the best result with an extra insertion loss of about zero. It indicates that the extra loss could be improved with maturity and practice of the assembly. The insertion loss at wavelength of $1570\ \text{nm}$ is better than that at wavelength of $1550\ \text{nm}$.

Table 3 and Figure 9 show data collected for each EAM module.

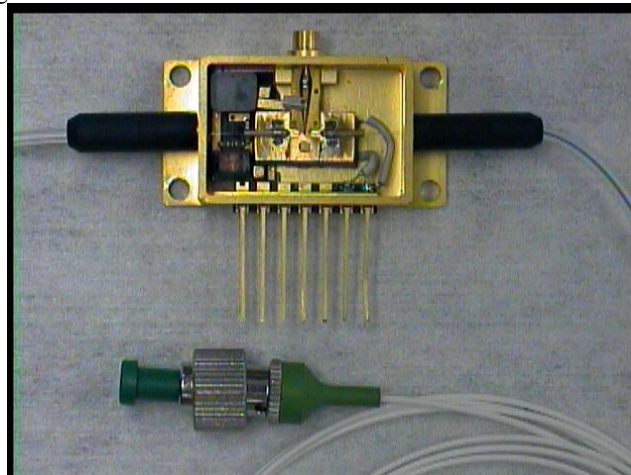


Figure 8: A picture of EAM module with fiber connector

Table 2: The summary of the insertion loss before and after the assembly

EAM module	Insertion loss (db)					
	19	24	27	28	30	108
Bench test @1550 nm	6.1	6.8	6.8	6.0	6.4	6.1
Final test @1550 nm	8.7	8.2	6.8	7.2	7.4	7.2
Final test @1570 nm	7.0	7.2	5.4	5.4	6.8	6.2

Table 3: Detailed information about device 28, typical of data taken for all modules.

	Test condition	@1550 nm	@1566 nm
Insertion loss	$P_{IN} = 0\text{dbm}$ $V_{DC} = 0\text{ V}$	7.1 db	5.4 db
Modulation depth	$P_{IN} = 0\text{dbm}$ $V_{DC} = 0 \sim -4\text{V}$	28 db	16 db

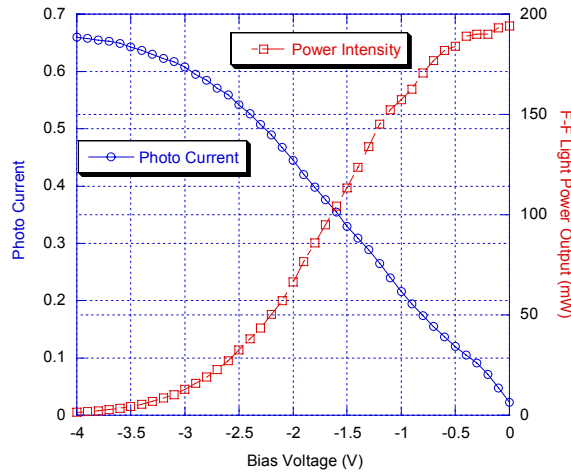


Figure 9: Photocurrent and Photointensity vs. Bias Voltage with the input power of 1 mw @1550nm

5. CONCLUSIONS

A dilute waveguide EAM device was designed in an effort to increase the maximum power and the dynamic range of the device. This design of the DCW EAM was intended to spatially separate the region of maximum photocurrent and photointensity. Using an optical test setup with a lensed fiber test method we show that the axes of maximum photocurrent and photointensity are separated by a distance of $\sim 0.4\text{ }\mu\text{m}$. Using these observations, an assembly process was developed for the DCW EAM.

Measurements are reported for six DCW EAM modules. The average insertion loss of the module is about 7.6 db. Improvements on this insertion loss are possible with the use of a lensed fiber with an optimized mode field. Based on data, we project that an improvement of 0.7 db is expected if we were to substitute lensed fiber with a mode field of $4\text{ }\mu\text{m}$ instead of the lensed fiber we used with a mode field of $3.3\text{ }\mu\text{m}$. We also expect that with the maturation of the assembly process, a final insertion of 6 db would be achievable for the PCW EAM in its packaged state.

6. REFERENCES

- [1] A. R. Williams, A. L. Kellner, and P. K. L. Yu, "Dynamic range performance of a high speed high saturation InGaAs/InP PIN waveguide photodetector" *Electronics Letters*, 31(7), 548-549 (1995).
- [2] H. Jiang, J.T.Zhu, A.L.Kellner, P.K. Yu, Y.Z. Liu, "High-saturation-power waveguide photodetector for analog fiber-optic links", *Proc. SPIE*, 2844, 120-124 (1996).
- [3] G.L. Li, S. A. Pappert, P Mages, C.K. Sun, W. S. C. Chang, P.K. L. Yu, "High-saturation high-speed traveling-wave InGaAsP-InP electroabsorption modulator," *Photonics Technology Letters, IEEE* , 13(10), 1076-1078 (2001).
- [4] P. Martin, E.M. Skouri, L. Chusseau, C. Albert, H. Bissessur, "Accurate refractive index measurements of doped and undoped InP by a grating coupling technique", *Appl. Phys. Lett.* 67, 881-883(1995).
- [5] N.Stoffel, S. Tan, C.Shick. W. Bacon, B. Beaman, A. Morrow, M. Green, R. Bussjager, S. Johns, M. Hayduk, J. Osman, R. Erdmann, B. McKeon, "Diamond Shaped Ring Laser Characterization, Package Design and Performance", *IEEE-ECTC*, 1583-1589(2006).